**SINERGI** Vol. 27, No. 2, June 2023: 241-248
http://publikasi.mercubuana.ac.id/index.php/sinergi
http://doi.org/10.22441/sinergi.2023.2.012

# The influence of heat rate and austenitization temperature on microstructure and hardness of Hadfield steel

**Haris Wahyudi[1*], Swandya Eka Pratiwi[1], Adolf Asih Supriyanto[2], Daisman Purnomo Bayyu Aji[3]**
[1]Department of Mechanical Engineering, Faculty of Engineering, Universitas Mercu Buana, Indonesia
[2]Mechatronics Engineering, Politeknik Enjinering Indorama, Indonesia
[3]Department of Mechanical Engineering, Universitas Trisakti, Indonesia

***Abstract***
*The As-Cast condition of Hadfield alloy usually contains (Fe, Mn)$_3$C carbides around the austenitic grains, which promote brittleness, making the steel impractical in industry. Heat treatment is normally applied to reduce carbide content, lower carbides, and improve toughness. However, a complete austenitic structure is not attainable during solution treatment. The dissolution temperature and dissolution time are critical to obtaining complete carbide content. Furthermore, heating must be done slowly, and the quenching speed must be fast enough. This study examines the effect of heat rate and austenitization temperatures in the solution treatment on the microstructure and hardness of Hadfield steel. The heat rate of 3, 6 and 10 °C/min is selected to determine whether there is a change in the microstructure of Hadfield steel. The four austenitization temperatures of 1000, 1100, 1150 and 1200 oC are used to ascertain carbide dissolution into the austenite matrix. Grain boundary, hardness, and phase transformation will confirm the microstructural change and hardness properties. The optical microscope shows carbide content is reduced as the austenitization temperature increases. The consequence of carbide dissolution affects the hardness. Its hardness decreases as temperature increase due to the loss of carbide. The as-Cast specimen has the highest hardness of 227.8 HV30, and the lowest hardness is 176.7 HV30 belongs to a specimen that is heated up to 1200 °C and quenched into water. Grain size is measured by the line intercept method, which shows its increase as temperatures increase. The result of grain measurement is as follows: As-Cast 224.6 μm, T 1000 °C 323.3 μm, T1100 °C 409.2 μm, T1150 °C 1014.4 μm, T1200 °C 881.6 μm. SEM-EDS confirms that the main phase is austenite, and a small amount of carbide is detected in the austenite matrix.*



***Keywords:***
*Austenitization temperature;*
*Carbide;*
*Hadfield steel;*
*Heat treatment;*
*Solution treatment;*

***Article History:***
*Received: September 1, 2022*
*Revised: December 13, 2022*
*Accepted: December 22, 2022*
*Published: June 2, 2023*

***Corresponding Author:***
*Haris Wahyudi*
*Mechanical Engineering Department, Universitas Mercu Buana, Indonesia*
*E-mail:*
*haris.wahyudi@mercubuana.ac.id*

## INTRODUCTION

Hadfield steel in the As-Cast condition usually contains (Fe, Mn)$_3$C carbides in the austenite matrix. It is a common industrial practice to have solution treatment the alloy before use so that (Fe, Mn)$_3$C dissolves into solution giving complete austenitic structure. Hadfield steel which consists mainly of 1.2 wt% C and 12 wt% Mn has attracted researchers to explore and examine it since the first invention by Robert Hadfield in 1882 [1]. Hadfield steel has austenite phase at room temperature, which has exceptionally good work hardening and wear resistance characteristics. This type of steel is widely used in in different industries such as mining, drilling, crusher, cement, and railway [2, 3, 4, 5].

Hadfield steels is manufactured by casting process, contain carbide $(Fe, Mn)_3C$ in the grain boundary due to slow solidification process [6, 7, 8, 9, 10, 11]. Figure1 shows the exemplary carbide precipitated in grain boundary. The precipitation of carbide at the grain boundary induces low toughness [12, 13, 14] and solution treatment of 1050-1200 ℃ follows by quenching process should be applied after casting in order to obtain the homogeneous austenitic structure [2, 6, 10, 13, 15, 16]. The solution treatment was conducted by [17][18] at temperatures of 1100 ℃, 1150 ℃ and 1200 ℃ for 40, 80 and 240 minutes, respectively. The higher the temperature the carbide content decrease dramatically. Different approach in solution treatment was used to achieve low carbide content [15] by heating Hadfield specimen at different temperature 970 ℃, 1060 ℃, 1150 ℃ and soaking time 30, 60 minutes. After reaching austenitization temperatures the specimens were directly quenched in choppy water. Two cycles processes [19, 20, 21] was performed in solution treatment, the initial temperature is 600 ℃ and then increased until 1020-1100 ℃.

Influence of temperature and soaking time is reported by [22][23]. They performed experiment on Hadfield steel using different temperature 1000 ℃, 1050 ℃ dan 1100 ℃ and soaking time of 1.5 hrs, 2 hrs and 3 hrs. After solution anneal the samples were quenched into water [24] and salt solution. Initially, carbides that is high at grain boundary gradually decrease as temperatures increase. Grain size was also bigger as soaking time prolonged.

The soaking time in austenitization temperatures determine the microstructures of Hadfield steel, increasing soaking time make the grains growth [15]. Soaking time of 240 minutes was still not produced austenite phase that free of carbide [17]. Initial pre-heat at 650 ℃ for 3 hours was intended to dissolve pearlite and later increase austenite transformation, increase carbon solution in the austenite matrix [10].

Heating rate of 6 ℃/min and 12 ℃/min was reported in [19], while the heating rate of 1.67 ℃/min and 75 ℃/h was addressed by [10] and [25], respectively. But the information of heating rate in obtaining fully austenite phase is insufficient.

Proper heat treatments to obtain a completely austenitic structure depend on four main parameters dissolution temperature, soaking time, heating rate and quenching medium. The first two parameters are critical, while the heating rate prevent internal crack and cooling speed must be sufficient to minimize carbide segregation [16].

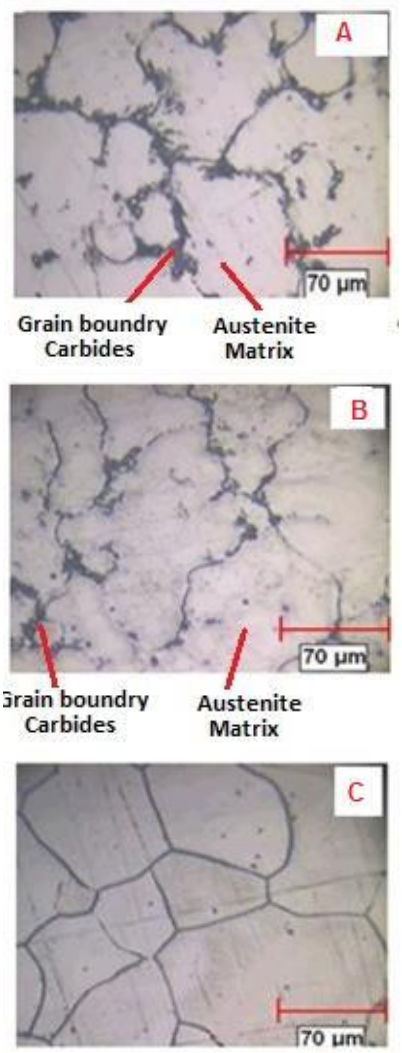


Figure 1. Optical micrograph of samples annelid at a). 970 ℃, b). 1060 ℃ and c). 1150 ℃ for 30 minutes [15]

However, the combination of the above parameters is dependent on the composition of Hadfield steel [26]. The primary purpose of this study was to determine the effect of solution treatment mainly heat rate and austenitization temperature in reducing carbides content and the hardness properties.

Here, the Hadfield samples were solution treated in tube furnace to obtain fully austenite phase and followed by water quenched. Subsequently, the microstructure and mechanical properties were analysed to understand the microstructure and property relationship.

## MATERIAL AND METHOD

The sample of Hadfield steel was produced by sand casting process, melted in induction furnace, and pouring temperature is about 1460 ℃. The mould is made of zircon sand

and the products have initial dimensions of 250 mm x 250 mm x 50 mm (width x length x depth). The Hadfield steel used in this study was selected from an Mn austenitic Hadfield steel of ASTM A-128 type C but lower Mn content. The composition of elements is characterized by Optical Emission Spectroscopy (OES) shown in Table 1.

To examine the simultaneous effects of the heating rate and austenitizing temperature the Hadfield steel structure, 8 samples was cut in the dimensions of 4x5x7 mm. Four samples were used for solution treatment with different heating rates and austenitization temperatures and another four samples for solution treatment. The design of experiment is shown in Table 2.

Samples S1-S8 were solution treated at different temperatures of 1000 ℃, 1100 ℃, 1150 ℃ and 1200 ℃ and the soaking time is 30 minutes, as presented in Figure2. At the end of the process, sample was quenched in water. Microstructure is observed by optical microscope after grinding and polishing, nital etched with 10-15 % solution followed by HCl 10% immersion for about one second. Heating rate treatments was controlled at 3, 6 and 10 ℃/min, fast quenching in water as well. Grinding was done using sandpaper with the mesh from 400-5000. Diamond paste and Colloidal silica was used for polishing.

Hardness measurements were made by micro-Vickers method model Future tech FV-810 with a load of 30 kgf. The hardness values were measured at three different point and the average of the hardness number is presented.

Microstructure of polished samples was observed using Optical Microscopy (OM) using Keyence VHZST. SEM-EDS model JEOL JSM IT-100 was used to identify microstructure and phase qualitatively.

Table 1. Hadfield steel composition (wt%)

| C | Mn | Cr | Si (max) | P (max) | Fe |
|---|---|---|---|---|---|
| 1.23 | 10.61 | 2.12 | 0.4 | 0.035 | Bal |

Table 2. Different specimens of Hadfield steel with different solution treatment processes

| No | Austenitization temperature, Tγ (˚C) | Heat rate (˚C/min) | Soaking time (min) |
|---|---|---|---|
| As-Cast | - | - | - |
| S1 | 1000 | 10 | 30 |
| S2 | 1100 | 10 | 30 |
| S3 | 1150 | 10 | 30 |
| S4 | 1200 | 10 | 30 |
| S5 | 1150 | 3 | 30 |
| S6 | 1150 | 6 | 30 |
| S7 | 1200 | 3 | 30 |
| S8 | 1200 | 6 | 30 |

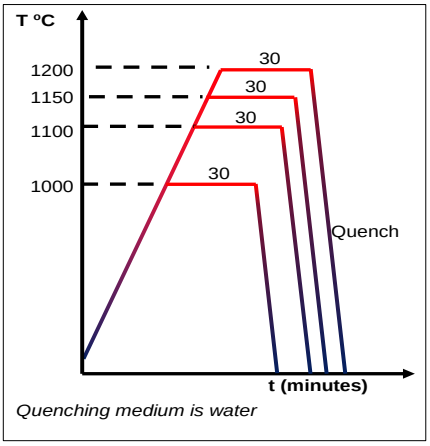


Figure 2. Illustration of solution treatment process

## RESULTS AND DISCUSSION

Figure3 shows optical microscopy of As-Cast Hadfield steel and solution treated samples at different austenitization temperatures. The magnification is 200x and the scale of all images is 250 μm, but the scale for As-Cast image is 150 μm to depict a larger area. The heat rate used for samples S1-S4 was 10 ℃/min. Figure 3(a) shows that the As-Cast sample consist of the austenite matrix and non-dissolved carbides at grain boundary as similarly reported by previous researchers [9, 10, 15, 18]. Figure 3(b)–3(e) display the effect austenitization temperature of Hadfield steel observed under optical microscope. The bright colour represents the austenite matrix while the black spot or area represents carbides. Hadfield steel mainly consists of austenite phase due to high concentrations of carbon and manganese. Carbide was formed due to the presence of high carbon and carbide forming elements such as Mn and Cr. Most carbide precipitate along grain boundary during slow solidification process.

Figure 3(b) exhibit microstructure of Hadfield steel after solution treatment at Tγ 1000 ℃. The presence of carbides is still frequent, but grain size is increased compared to As-Cast sample. Due to high percentage of Cr (> 2 wt%), it stabilized carbide formation.

Higher solution treatment temperature for Hadfield steel is necessary prior to water quenching [6]. As austenitization temperature increased (1100- 1200 ℃) the number of carbides decrease but the grain size coarser as illustrated in Figure 3(c) – 3(e).

The influence of heating rate is depicted in Figure 4(a) – 4(d). It is confirmed that the heating rate of 3 ℃/min and 6 ℃/min did not produce internal crack.

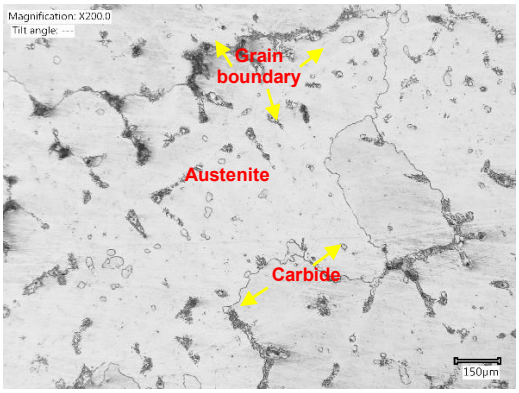


a). OM images of sample As-Cast

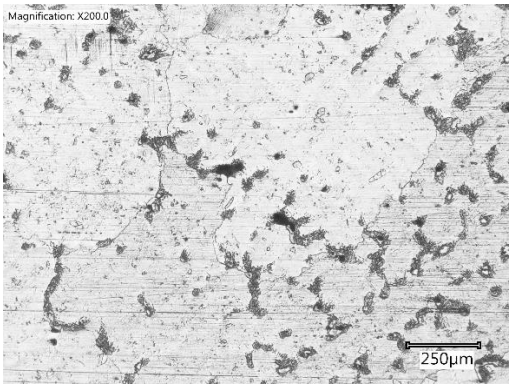


b). OM images of sample S1, Tγ 1000 ℃

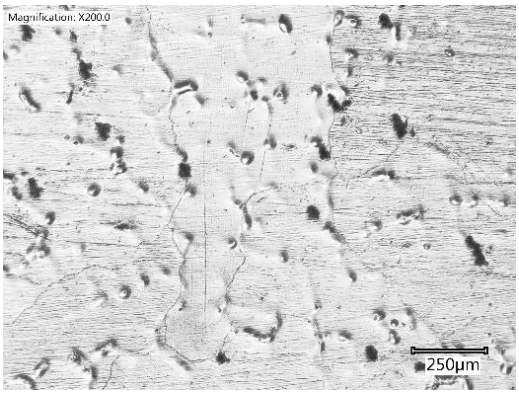


c). OM images of sample S2, Tγ 1100 ℃

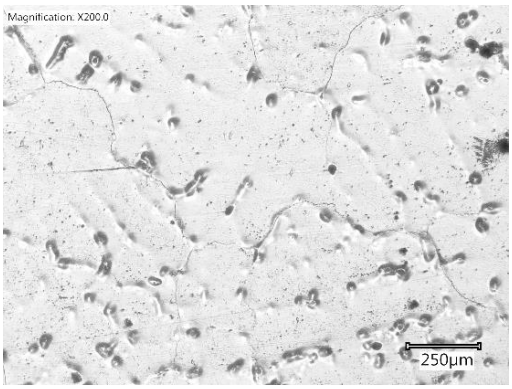


d). OM images of sample S3, Tγ 1150 ℃

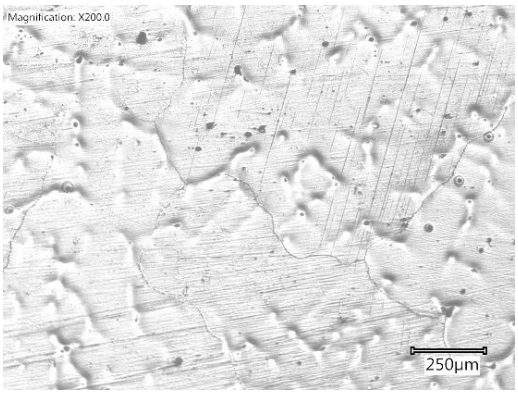


e). OM images of sample S4, Tγ 1200 ℃

Figure 3. Optical Microscopy (OM) of the Hadfield steel samples at different austenitization temperatures a). As-Cast, b). Tγ 1000 ℃, c). Tγ 1100, d). Tγ 1150 ℃, e). Tγ 1200 ℃

At lower heating rate, 3 ℃/min, the number of carbides is lesser compared to samples that have been heated at higher heating rate 6 ℃/min). It is because the time of carbon dissolution is sufficient to dissolve into the austenite matrix, slower heating rate affect the growth of grain and produces bigger grain size.

SEM-EDS was performed for the sample As-Cast and sample S4 which was solution treated at 1200 ℃. Figure 5 and Figure 6 shows the selected points (Point A to Point F) from SEM to identify the element and carbide distribution of As-Cast and S4 sample, respectively.

EDS Map sum spectrum of As-Cast is shown in Figure 7 and EDS Map sum spectrum of S4 sample is shown and Figure 8. EDS spectrum result showing the individual element of As-Cast and S4 sample is summarised in Table 3 and Table 4.

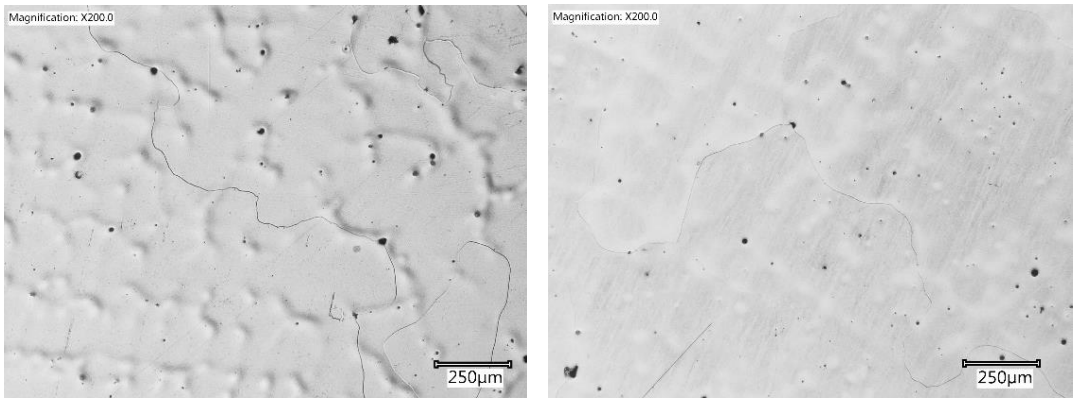


a). OM images of sample S5, Tγ1150 ℃, 3 ℃/min b). OM images of sample S6, Tγ 1150 ℃ 6 ℃/min

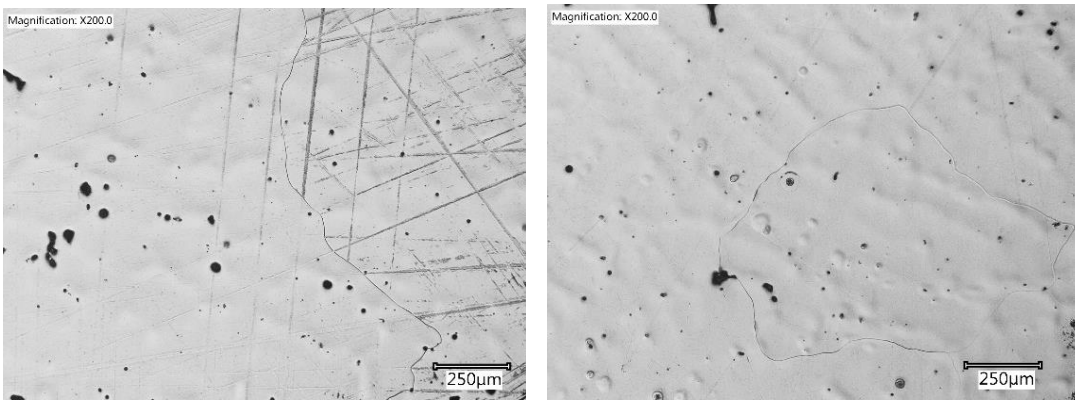


c). OM images of sample S7, Tγ 1200 ºC 3 ℃/min d). OM images of sample S8, Tγ 1200 ℃ 6 ℃/min

Figure 4. Optical micrograph heat treated at different Tγ and heating rate a). Tγ1150 ℃, 3 ℃/min, b). Tγ 1150 ℃ 6 ℃/min, c). Tγ 1200 ℃ 3 ℃/min, d). Tγ 1200 ℃ 6 ℃/min

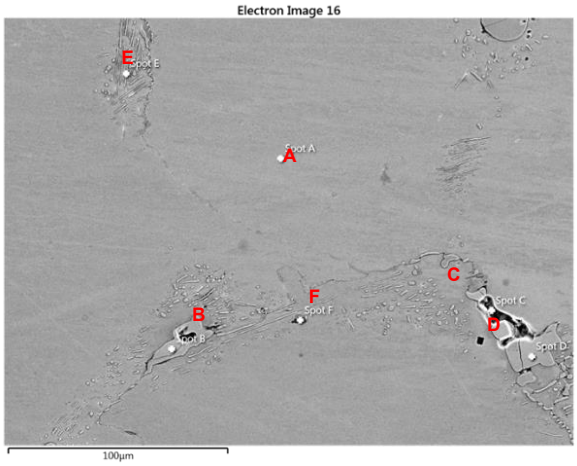


Figure 5. SEM of As-Cast sample

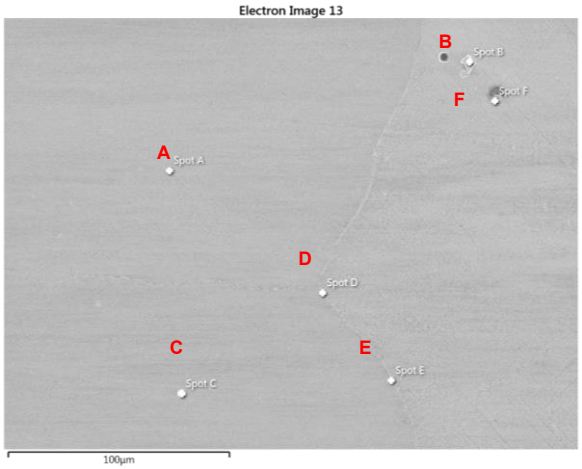


Figure 6. SEM of sample S4 (Tγ 1200 ℃)

Comparing Figure 5 and Figure 6 confirms that carbide content is reduce from As-Cast state and solution treated. Carbides are apparently seen at the grain boundary, as shown in Figure 5, compared to Figure 6. The carbide forming element (e.g., Mn, Cr) lessens As-Cast to S4 sample, as indicated in Table 3 and Table 4.

Grain size result of the samples is depicted in Figure 9. Grain size is measured by line intercept method and the result show its increase as temperatures increases [16]. As-Cast sample has the smallest grain size of 224.6 µm. Sample S1 has the grain size value of 323.3 µm, S2 409.2 µm. S3 1014.4 µm and S4 881.6 µm.

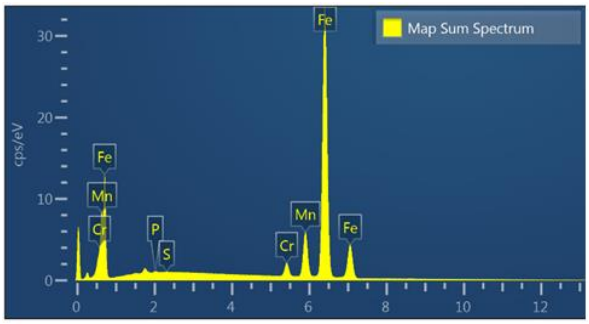


Figure 7. EDS Map sum spectrum for As-Cast sample

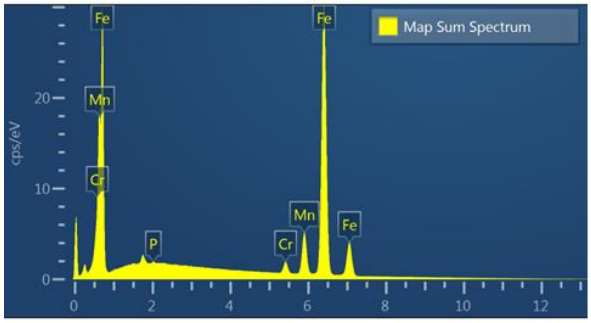


Figure 8. EDS Map sum spectrum for S4 sample

Table 3. EDS spectrum result of As-Cast sample

| Element | Spot A | | Spot B | | Spot C | |
|---|---|---|---|---|---|---|
| | wt% | at% | wt% | at% | wt% | at% |
| Fe | 83.8 | 69.99 | 61.1 | 44.71 | 53.29 | 23.56 |
| Mn | 9.08 | 7.71 | 19.96 | 14.84 | 6.73 | 3.03 |
| C | 5.3 | 20.59 | 9.75 | 33.18 | 33.98 | 69.85 |
| Cr | 1.7 | 1.52 | 9.08 | 7.14 | 3.69 | 1.75 |
| P | 0.1 | 0.15 | 0.05 | 0.07 | 1.36 | 1.08 |
| S | 0.02 | 0.03 | 0.05 | 0.07 | 0.95 | 0.73 |
| Total | 100 | 100 | 100 | 100 | 100 | 100 |

| Element | Spot D | | Spot E | | Spot F | |
|---|---|---|---|---|---|---|
| | wt% | at% | wt% | at% | wt% | at% |
| Fe | 60.75 | 45.64 | 74.37 | 10.28 | 11.11 | 6.36 |
| Mn | 20.07 | 15.33 | 13.37 | 2.76 | 47.71 | 27.74 |
| C | 8.74 | 30.52 | 8.65 | 56.25 | 15.28 | 40.63 |
| Cr | 10.27 | 8.29 | 3.4 | 30.43 | 1.43 | 0.88 |
| P | 0.06 | 0.08 | 0.16 | 0.22 | 0 | 0 |
| S | 0.11 | 0.14 | 0.05 | 0.06 | 24.48 | 24.39 |
| Total | 100 | 100 | 100 | 100 | 100 | 100 |

The grain size increase as austenitization temperature increase due to grain growth mechanisms. The grain size affects the strength (yield stress) of metallic materials as well as Hadfield steel, the theory by the Hall-Petch equation [27][28]. Smaller grain hinders the deformation mechanism by dislocation or twin. Smaller grain size contributes to the higher hardness of Hadfield steel as shown in Figure 10.

The hardness distribution of samples is presented in Figure 10. From left to right the hardness tends to decrease. The carbide is hard compared to austenite phase. As carbide decrease the hardness of sample is decreased as well.

Table 4. EDS spectrum result of sample S4 (Tγ 1200 °C)

| Element | Spot A | | Spot B | | Spot C | |
|---|---|---|---|---|---|---|
| | wt% | at% | wt% | at% | wt% | at% |
| Fe | 86.3 | 79.42 | 80.03 | 72.12 | 85.45 | 77.19 |
| Mn | 9.69 | 9.06 | 13.73 | 12.58 | 9.85 | 9.05 |
| C | 2.27 | 9.72 | 2.88 | 12.06 | 2.82 | 11.84 |
| Cr | 1.62 | 1.61 | 3.36 | 3.25 | 1.71 | 1.66 |
| P | 0.12 | 0.19 | 0 | 0 | 0.13 | 0.21 |
| S | 0 | 0 | 0 | 0 | 0.04 | 0.06 |
| Total | 100 | 100 | 100 | 100 | 100 | 100 |

| Element | Spot D | | Spot E | | Spot F | |
|---|---|---|---|---|---|---|
| | wt% | at% | wt% | at% | wt% | at% |
| Fe | 85.17 | 76.94 | 84.98 | 76.94 | 78.08 | 64.87 |
| Mn | 10.03 | 9.21 | 10.31 | 9.49 | 13.09 | 11.05 |
| C | 2.81 | 11.82 | 2.76 | 11.61 | 5.22 | 20.18 |
| Cr | 1.82 | 1.77 | 1.86 | 1.81 | 2.4 | 2.14 |
| P | 0.13 | 0.21 | 0.08 | 0.13 | 0.2 | 0.31 |
| S | 0.03 | 0.04 | 0.02 | 0.02 | 1 | 1.45 |
| Total | 100 | 100 | 100 | 100 | 100 | 100 |

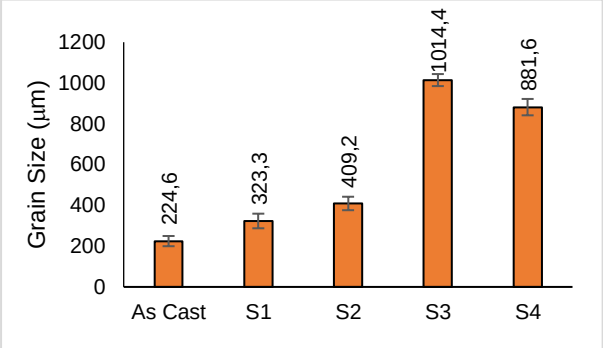


Figure 9. Grain size distribution of samples from left to right: As-Cast, S1, S2, S3 and S4

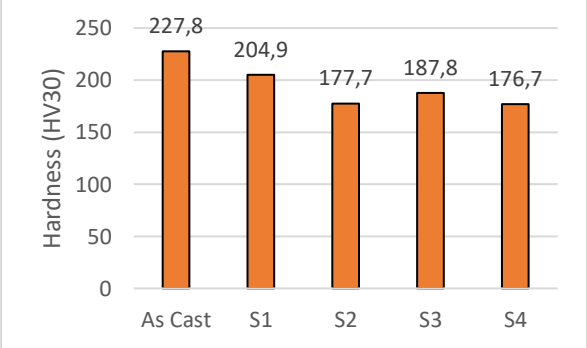


Figure 10. Hardness result of samples from left to right: As-Cast, S1, S2, S3 and S4

Analysis also found that this trend relevant with the grain size distribution. The hardness of As-Cast and solution-treated samples is averaged as follows As-Cast 227.8 HV30, Tγ 1000 °C 204,9 HV30, Tγ 1100 °C 177,7 HV30, Tγ 1150 °C 187,8 HV30 dan Tγ 1200 °C 176,7 HV30.

## CONCLUSION

From the results of the experiment, it can be concluded that as follows. The increasing solution

treatment temperatures from 1000, 1100, 1150 and 1200 ℃ dissolve more carbides of the Hadfield steel into austenite matrix. It is quite apparent from the microstructure of the As-Cast alloys that is consisted of an austenite matrix with carbides along the grain boundaries. The grain size increase as austenitization temperature increase. As-Cast sample has the smallest grain size of 224.6 μm and at austenitization temperature of 1000, 1100, 1150 and 1200 ºC, the grain size is 323.3 μm, 409.2 μm, 1014.4 μm and 881.6 μm, respectively. The decrease in hardness was influenced by the morphology and distribution of the carbides in the As-Cast and solution treated samples. As-Cast has the highest hardness 227.8 HV30. It decreases as austenitization temperatures decrease: Tγ 1000 ℃ 204,9 HV30, Tγ 1100 ℃ 177,7 HV30, Tγ 1150 ℃ 187,8 HV30 dan Tγ 1200 ℃ 176,7 HV30.

## ACKNOWLEDGMENT

The authors would like to thank to Universitas Mercu Buana for their support through the funding of this research.

## REFERENCES

[1] Joseph D. Weeks, “Hadfield’s Manganese Steel,” *Science (1979)*, vol. ns-12, no. 306, pp. 284–284, 1888, doi: 10.1126/science.ns-12.306.284.

[2] M. Sabzi and M. Farzam, “Hadfield manganese austenitic steel: A review of manufacturing processes and properties,” *Materials Research Express*, vol. 6, no. 10, 2019, doi: 10.1088/2053-1591/ab3ee3.

[3] R. Jacob, S. Raman Sankaranarayanan, and S. P. Kumaresh Babu, “Recent advancements in manganese steels-A review,” in *Materials Today: Proceedings*, vol. 27, no. 3, pp. 2852-2858, 2019. doi: 10.1016/j.matpr.2020.01.296.

[4] Y. Gao, P. Wang, Y. Liu, J. Xu, Z. Dong, and K. Wang, “Investigation on wheel-rail contact and damage behavior in a flange bearing frog with explicit finite element method,” *Mathematical Problems in Engineering*, vol. 2019, 2019, doi: 10.1155/2019/1209352.

[5] R. A. Al-Samarai and H. Haftirman, “Tribological properties of Al2o3-Zro2 composite coating by lubrication,” *SINERGI*, vol. 25, no. 3, pp. 371–380, Aug. 2021, doi: 10.22441/sinergi.2021.3.014.

[6] D. K. Subramanyam, A. E. Swansiger, and H. S. Avery, “Austenitic Manganese Steel,” in *ASM Handbook, Volume 1, Properties and Selection: Irons, Steels, and High Performance Alloys*, 2005, pp. 1274–1302. doi: 10.31399/asm.hb.v01.a0001045.

[7] Q. Q. Ren, T. Liu, S. Il Baik, Z. Mao, B. W. Krakauer, and D. N. Seidman, “The effects of alloying elements on the peritectic range of Fe–C–Mn–Si steels,” *Journal of Materials Science*, vol. 56, no. 10, pp. 6448-6464, 2021, doi: 10.1007/s10853-020-05602-6.

[8] T. Cao, C. Cheng, F. Ye, H. Xv, and J. Zhao, “Relationship between carbon segregation and the carbide precipitation along grain boundary based on the structural unit model,” *Journal of Materials Science*, vol. 55, pp. 7883-7893, 2020, doi: 10.1007/s10853-020-04537-2.

[9] S. Ayadi and A. Hadji, “Effect of Chemical Composition and Heat Treatments on the Microstructure and Wear Behavior of Manganese Steel,” *International Journal of Metalcasting*, vol. 15, no. 2, pp. 510-519, 2021, doi: 10.1007/s40962-020-00479-2.

[10] U. Gürol and S. C. Kurnaz, “Effect of carbon and manganese content on the microstructure and mechanical properties of high manganese austenitic steel,” *Journal of Mining and Metallurgy, Section B: Metallurgy*, vol. 56, no. 2, 2020, doi: 10.2298/JMMB191111009G.

[11] T. Dement, N. Popova, and I. Kurzina, “Influence of the C and Mn concentration on the grains size of the Fe-Mn-C alloy,” in *AIP Conference Proceedings*, 2016. doi: 10.1063/1.4964553.

[12] Y. S. Ham, J. T. Kim, S. Y. Kwak, J. K. Choi, and W. Y. Yoon, “Critical cooling rate on carbide precipitation during quenching of austenitic manganese steel,” *China Foundry*, vol. 7, no. 2, pp. 178–182, 2010.

[13] S. Mishra and R. Dalai, “A comparative study on the different heat-treatment techniques applied to high manganese steel,” in *Materials Today: Proceedings*, 2021. doi: 10.1016/j.matpr.2020.12.602.

[14] A. A. Mohamed, M. K. El-fawkhry, and W. M. El-nahas, “The Effect of Precipitation Hardening on the Properties Hadfield Steel,” *ERJ. Engineering Research Journal*, vol. 43, no. 2, pp. 119–125, Apr. 2020, doi: 10.21608/erjm.2020.83899.

[15] M. Beheshti, M. Zabihiazadboni, M. C. Ismail, S. Kakooei, and S. Shahrestani, “Investigation on Simultaneous Effects of Shot Peen and Austenitizing Time and Temperature on Grain Size and Microstructure of Austenitic Manganese Steel (Hadfield),” in *IOP Conference Series: Materials Science and Engineering 328*, 2018, pp. 1–8. doi: 10.1088/1757-899X/328/1/012006.

[16] H. R. Jafarian, M. Sabzi, S. H. Mousavi Anijdan, A. R. Eivani, and N. Park, "The influence of austenitization temperature on microstructural developments, mechanical properties, fracture mode and wear mechanism of Hadfield high manganese steel," *Journal of Materials Research and Technology*, vol. 10, pp. 819-831, 2021, doi: 10.1016/j.jmrt.2020.12.003.

[17] G. Tęcza and S. Sobula, "Effect of Heat Treatment on Change Microstructure of Cast High-manganese Hadfield Steel with Elevated Chromium Content," *Archives of Foundry Engineering*, vol. 14, no. 3, pp. 67–70, 2014.

[18] R. Zellagui *et al.*, "Effect of Heat Treatments on the Microstructure, Mechanical, Wear and Corrosion Resistance of Casted Hadfield Steel," *International Journal of Metalcasting*, vol. 16, no. 2, 2022, doi: 10.1007/s40962-021-00751-z.

[19] S. Ayadi and A. Hadji, "Effect of heat treatments on the microstructure and wear resistance of a modified hadfield steel," *Metallofizika i Noveishie Tekhnologii*, vol. 41, no. 5, 2019, doi: 10.15407/mfint.41.05.0607.

[20] B. Bandanadjaja and E. Hidayat, "The effect of two-step solution heat treatment on the impact properties of Hadfield austenitic manganese steel," in *Journal of Physics: Conference Series*, 2020. doi: 10.1088/1742-6596/1450/1/012125.

[21] M. Azadi, A. M. Pazuki, and M. J. Olya, "The Effect of New Double Solution Heat Treatment on the High Manganese Hadfield Steel Properties," *Metallography, Microstructure, and Analysis*, vol. 7, no. 3, 2018, doi: 10.1007/s13632-018-0471-0.

[22] S. Hosseini, M. B. Limooei, M. H. Zade, E. Askarnia, and Z. Asadi, "Optimization of Heat Treatment Due to Austenising Temperature, Time and Quenching Solution in Hadfield Steels," *International Journal of Materials and Metallurgical Engineering*, vol. 7, no. 7, pp. 582–585, 2013, doi: doi.org/10.5281/zenodo.1087486.

[23] S. A. Torabi, K. Amini, and M. Naseri, "Investigating the Effect of Manganese Content on the Properties of High Manganese Austenitic Steels," *International Journal of Advanced Design and Manufacturing Technology*, vol. 10, no. 1, pp. 75–83, 2017.

[24] M. Rohmah, P. A. Paristiawan, and T. B. Romijarso, "Effect of forging load and heat treatment process on the corrosion behavior of A588-1%NI for weathering steel application in a marine environment," *SINERGI*, vol. 26, no. 2, pp. 237-248, Jun. 2022, doi: 10.22441/sinergi.2022.2.013.

[25] Z. Zhou, Z. Zhang, Q. Shan, Z. Li, Y. Jiang, and R. Ge, "Influence of heat-treatment on enhancement of yield strength and hardness by Ti-V-Nb alloying in high-manganese austenitic steel," *Metals (Basel)*, vol. 9, no. 3, 2019, doi: 10.3390/met9030299.

[26] H. Wahyudi, T. Dirgantara, R. Suratman, and A. Ramelan, "Pengaruh Faktor dan Mekanisme Pengerasan Regangan pada Baja Hadfield," *MESIN*, vol. 27, no. 2, pp. 40–54, 2018.

[27] Y. P. Asmara, "Simulation of CO2 Corrosion of Carbon Steel in High Pressure and High Temperature Environment," *Journal of Integrated and Advanced Engineering (JIAE),* vol. 2, no. 1, pp. 63-70, 2022, doi: 10.5162/jiae.v2i1.40

[28] W. D. J. Callister and D. G. Rethwisch, *Materials Science and Engineering: An Introduction Seventh Edition*. 2007. doi: 10.1016/0025-5416(87)90343-0.